

# Army Research Laboratory

Aberdeen Proving Ground, MD 21005-5066

---

---

ARL-CR-456

July 2000

---

---

## Simulation of Two Projectiles Connected by a Flexible Tether

Mark F. Costello and Geoffrey W. Frost  
Oregon State University

---

---

## Abstract

---

This report investigates the atmospheric flight mechanics of two projectiles connected by a flexible tether. Both projectiles are individually modeled with six degrees of freedom. The projectile aerodynamic model depends on angle of attack and Mach number and includes unsteady roll, pitch, and yaw aerodynamic damping. The tether is split into a finite number, of beads, with each bead possessing three translation degrees of freedom. Forces acting on the beads include weight, line stiffness, line damping, and aerodynamic drag. The tether aerodynamic drag force is dependent on the tether line angle of attack and Mach number. The tether line deployment process is modeled with a single degree of freedom that permits unreeling resistance to be incorporated. The effect of follower-to-lead projectile mass ratio and drag coefficient ratio on system response are investigated.

# Table of Contents

	<u>Page</u>
<b>List of Figures</b> .....	v
<b>1. Introduction</b> .....	1
<b>2. Projectile Mathematical Models</b> .....	2
<b>3. Tether Mathematical Model</b> .....	4
3.1 Elastic Line Forces .....	6
3.2 Aerodynamic Line Forces .....	7
<b>4. Reel Dynamic Model</b> .....	8
<b>5. Flight Phases</b> .....	9
<b>6. Results</b> .....	9
<b>7. Conclusions</b> .....	17
<b>8. References</b> .....	23
<b>List of Symbols</b> .....	25
<b>Distribution List</b> .....	27
<b>Report Documentation Page</b> .....	33

INTENTIONALLY LEFT BLANK.

## List of Figures

<u>Figure</u>	<u>Page</u>
1. Tether Bead Model Schematic .....	5
2. Deployment Schematic.....	10
3. Range (Mass Ratio = 1%, 100%) .....	12
4. Pitch Angle (Lead/Follower, Mass Ratio = 1%, 100%) .....	12
5. Body Forward Velocity (Lead/Follower, Mass Ratio = 1%, 100%) .....	13
6. Pitch Rate (Lead/Follower, Mass Ratio = 1%, 100%) .....	13
7. Angle of Attack (Lead/Follower, Mass Ratio = 1%, 100%) .....	14
8. Range (Lead/Follower, Mass Ratio = 100%, Drag Coefficient Ratio = 1.25, 1.5, 1.75, 2).....	15
9. Pitch Angle (Lead/Follower, Mass Ratio = 100%, Drag Coefficient Ratio = 1.25, 1.5, 1.75, 2).....	15
10. Lead Forward Velocity (Mass Ratio = 100%, Drag Coefficient Ratio = 1.25, 1.5, 1.75, 2).....	16
11. Follower Forward Velocity (Mass Ratio = 100%, Drag Coefficient Ratio = 1.25, 1.5, 1.75, 2).....	16
12. Tether Line Out Rate (Mass Ratio = 100%, Drag Coefficient Ratio = 1.25, 1.5, 1.75, 2).....	17
13. Tether Line Out (Mass Ratio = 100%, Drag Coefficient Ratio = 1.25, 1.5, 1.75, 2).....	18
14. Range (Mass Ratio = 1%, Drag Coefficient Ratio = 1.0625, 1.125, 1.25, 1.5, 1.75, 2).....	18
15. Pitch Angle (Lead/Follower, Mass Ratio = 1%, Drag Coefficient Ratio = 1.0625, 1.125, 1.25, 1.5, 1.75, 2).....	19

Figure

Page

16.	Lead Forward Velocity (Mass Ratio = 1%, Drag Coefficient Ratio = 1.0625, 1.125, 1.25, 1.5, 1.75, 2).....	19
17.	Follower Forward Velocity (Mass Ratio = 1%, Drag Coefficient Ratio = 1.0625, 1.125, 1.25, 1.5, 1.75, 2).....	20
18.	Tether Line Out Rate (Mass Ratio = 1%, Drag Coefficient Ratio = 1.0625, 1.125, 1.25, 1.5, 1.75, 2).....	20
19.	Tether Line Out (Mass Ratio = 1%, Drag Coefficient Ratio = 1.0625, 1.125, 1.25, 1.5, 1.75, 2).....	21

# 1. Introduction

Coupling two flight vehicles with a tether is by no means new, and a considerable bulk of literature has amassed. For example, Tye and Han [1], Puig-Suari, Longuski, and Tragesser [2], and No and Cochran [3] provide examples of tethers used for spacecraft applications. Phillips [4] and Clifton et al. [5] address the application of tethers to atmospheric flight vehicles. Djerassi and Viderman [6] investigated the motion of two bodies connected by a cable in atmospheric free fall, and in particular, focused on a device to terminate a missile launch in flight. Upon mission abort, a missile would be separated into a stable lead projectile and an unstable follower projectile, with the purpose of drastically reducing range in a predictable manner. The cable length was assumed short so that elastic collisions between the two bodies occurred; this, in turn, induced relatively large yaw angle excursions and resulted in reduced range.

The current effort develops a dynamic model of two projectiles connected by a flexible tether. Each projectile is modeled as a rigid body with six degrees of freedom. Loads on each projectile include weight and aerodynamic forces. The aerodynamic forces and moments are a function of the attack angle of the axis of symmetry of the projectile and the Mach number at the center of gravity. The aerodynamic expansion includes terms for high angle of attack flight as well as terms for roll, pitch, and yaw unsteady aerodynamic damping. Motion of the two projectiles is coupled through a tether line. The tether line is connected to each body with a frictionless ball-and-socket joint at an arbitrary point. The tether line is modeled as an elastic body, and is split into a finite number of beads; each bead is a point mass consisting of three translation degrees of freedom. Forces that drive the motion of the beads include bead weight, line spring force, line damping force, and aerodynamic drag. The tether line aerodynamic drag force is a function of the attack angle of the tether line and the local Mach number of the tether line element. The tether line deployment process is governed by a single degree of freedom model, which allows tether reel resistance to be incorporated.

## 2. Projectile Mathematical Models

The mathematical model describing the motion of both projectiles allows for six rigid-body degrees of freedom comprised of three body inertial position coordinates as well as three Euler angle body attitudes. This mathematical model has been validated against spark range data for a generic 25-mm, fin-stabilized sabot launched projectile [7]. Agreement between the model and range data is excellent.

The equations presented below use the ground surface as an inertial reference frame. The body frame is defined in the conventional manner [8], and the dynamic equations are written with respect to this coordinate system. The translation and rotation kinematic and dynamic equations for the lead projectile are given by equations (1–4) [8, 9].

$$\begin{Bmatrix} \dot{x}_L \\ \dot{y}_L \\ \dot{z}_L \end{Bmatrix} = [T_{L/I}] \begin{Bmatrix} u_L \\ v_L \\ w_L \end{Bmatrix}, \quad (1)$$

$$\begin{Bmatrix} \dot{\phi}_L \\ \dot{\theta}_L \\ \dot{\psi}_L \end{Bmatrix} = \begin{bmatrix} 1 & s_{\phi_L} t_{\theta_L} & c_{\phi_L} t_{\theta_L} \\ 0 & c_{\phi_L} & -s_{\phi_L} \\ 0 & s_{\phi_L} / c_{\theta_L} & c_{\phi_L} / c_{\theta_L} \end{bmatrix} \begin{Bmatrix} p_L \\ q_L \\ r_L \end{Bmatrix}, \quad (2)$$

$$\begin{Bmatrix} \dot{u}_L \\ \dot{v}_L \\ \dot{w}_L \end{Bmatrix} = \begin{Bmatrix} X_L / m_L \\ Y_L / m_L \\ Z_L / m_L \end{Bmatrix} - [S_L] \begin{Bmatrix} u_L \\ v_L \\ w_L \end{Bmatrix}, \text{ and} \quad (3)$$

$$\begin{Bmatrix} \dot{p}_L \\ \dot{q}_L \\ \dot{r}_L \end{Bmatrix} = [I_L]^{-1} \left[ \begin{Bmatrix} L_L \\ M_L \\ N_L \end{Bmatrix} - [S_L][I_L] \begin{Bmatrix} p_L \\ q_L \\ r_L \end{Bmatrix} \right]. \quad (4)$$

The follower projectile equations are identical in structure to the previous equations, but are omitted here due to space limitations. The matrix  $[T_{LI}]$  represents the transformation from the lead projectile body frame to the inertial frame. The matrix  $[S_L]$  is the skew symmetric cross product operator on the lead projectile body angular velocity components.

The total applied forces on the lead projectile is split into contributions due to the tether line (T), weight (W), and body aerodynamics (A).

$$\begin{Bmatrix} X_L \\ Y_L \\ Z_L \end{Bmatrix} = \begin{Bmatrix} X_{LT} \\ Y_{LT} \\ Z_{LT} \end{Bmatrix} + \begin{Bmatrix} X_{LW} \\ Y_{LW} \\ Z_{LW} \end{Bmatrix} - \begin{Bmatrix} X_{LA} \\ Y_{LA} \\ Z_{LA} \end{Bmatrix},$$

where

$$\begin{Bmatrix} X_{LW} \\ Y_{LW} \\ Z_{LW} \end{Bmatrix} = W_L \begin{Bmatrix} -s_{\theta_L} \\ s_{\phi_L} c_{\theta_L} \\ c_{\phi_L} c_{\theta_L} \end{Bmatrix}, \text{ and}$$

$$\begin{Bmatrix} X_{LA} \\ Y_{LA} \\ Z_{LA} \end{Bmatrix} = \frac{1}{2} \rho_L V_L^2 D_L \begin{Bmatrix} C_{X0}^L + C_{XA2}^L \alpha_L^2 + C_{XB2}^L \beta_L^2 \\ C_{Y0}^L + C_{YB1}^L \beta_L \\ C_{Z0}^L + C_{ZA1}^L \alpha_L \end{Bmatrix}. \quad (5)$$

The total applied body moments contain contributions from the tether line (T), steady body aerodynamics (SA), and unsteady body aerodynamics (UA).

$$\begin{Bmatrix} L_L \\ M_L \\ N_L \end{Bmatrix} = \begin{Bmatrix} L_{LT} \\ M_{LT} \\ N_{LT} \end{Bmatrix} + \begin{Bmatrix} L_{LSA} \\ M_{LSA} \\ N_{LSA} \end{Bmatrix} + \begin{Bmatrix} L_{LUA} \\ M_{LUA} \\ N_{LUA} \end{Bmatrix}. \quad (6)$$

The projectiles considered in the subsequent analysis are spin-stabilized with relatively low roll rates, so Magnus effects were not included in the aerodynamic expansion. The steady body aerodynamic moment is computed by a cross product between the distance vector from the center of gravity to the center of pressure and the steady body aerodynamic force vector. The unsteady body aerodynamic moment provides a damping source for projectile angular motion and is given.

$$\begin{Bmatrix} L_{LUA} \\ M_{LUA} \\ N_{LUA} \end{Bmatrix} = \frac{1}{2} \rho_L V_L^2 D_L^2 \begin{Bmatrix} C_{LDD}^L + \frac{p_L D_L C_{LP}^L}{2V_L} \\ \frac{q_L D_L C_{MQ}^L}{2V_L} \\ \frac{r_L D_L C_{NR}^L}{2V_L} \end{Bmatrix}. \quad (7)$$

The longitudinal and lateral aerodynamic angles of attack,  $\alpha_L$  and  $\beta_L$ , are computed using the following equations:

$$\alpha_L = \tan^{-1}\left(\frac{w_L}{u_L}\right) \text{ and } \beta_L = \tan^{-1}\left(\frac{v_L}{u_L}\right). \quad (8)$$

Air density is computed using the center of gravity position of the appropriate projectile in concert with the standard atmosphere [10]. The aerodynamic coefficients are Mach number dependent. Computationally, they are obtained by a table look-up scheme using linear interpolation. Mach number is computed at the center of gravity of the respective projectile.

### 3. Tether Mathematical Model

As depicted in Figure 1, the tether is split into  $N_b$  point mass elements and  $N_b + 1$  line elements. The motion of the point masses defines the motion of the tether line during deployment and throughout its flight phases. Each tether bead is a point mass possessing three translation

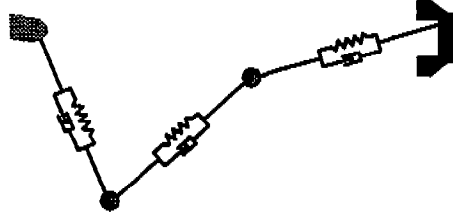


Figure 1. Tether Bead Model Schematic.

degrees of freedom. Forces that drive the motion of the tether beads include tether bead weight, adjacent tether line elastic forces, and tether bead aerodynamic forces. The tether bead equations of motion that follow are the same structurally for all beads, so the formulas are shown only for the  $i$ th tether bead. The equations are resolved in the inertial reference frame.

$$m_{T_i} \begin{Bmatrix} \ddot{x}_{T_i} \\ \ddot{y}_{T_i} \\ \ddot{z}_{T_i} \end{Bmatrix} = \begin{Bmatrix} X_{T_i} \\ Y_{T_i} \\ Z_{T_i} \end{Bmatrix} - \begin{Bmatrix} X_{T_{i+1}} \\ Y_{T_{i+1}} \\ Z_{T_{i+1}} \end{Bmatrix} + \begin{Bmatrix} X_A \\ Y_A \\ Z_A \end{Bmatrix} + \begin{Bmatrix} 0 \\ 0 \\ W_{T_i} \end{Bmatrix}. \quad (9)$$

In order to concisely express the different tether bead applied loads, the following tether bead position and velocity matrices are introduced:

$$R_T = \begin{bmatrix} R_1 \\ R_2 \\ \vdots \\ R_{N_B-1} \\ R_{N_B} \end{bmatrix} = \begin{bmatrix} x_L^* & y_L^* & z_L^* \\ x_{T_1} & y_{T_1} & z_{T_1} \\ \vdots & \vdots & \vdots \\ x_{T_{N_B}} & y_{T_{N_B}} & z_{T_{N_B}} \\ x_F^* & y_F^* & z_F^* \end{bmatrix}, \text{ and} \quad (10)$$

$$\dot{R}_T = \begin{bmatrix} \dot{R}_1 \\ \dot{R}_2 \\ \vdots \\ \dot{R}_{N_B-1} \\ \dot{R}_{N_B} \end{bmatrix} = \begin{bmatrix} \dot{x}_L^* & \dot{y}_L^* & \dot{z}_L^* \\ \dot{x}_{T_1} & \dot{y}_{T_1} & \dot{z}_{T_1} \\ \vdots & \vdots & \vdots \\ \dot{x}_{T_{N_B}} & \dot{y}_{T_{N_B}} & \dot{z}_{T_{N_B}} \\ \dot{x}_F^* & \dot{y}_F^* & \dot{z}_F^* \end{bmatrix}. \quad (11)$$

Equations (10) and (11) contain  $N_B + 2$  rows and three columns. The first and last row elements contain the inertial position and velocity of the lead and follower projectile/tether connection points.

**3.1 Elastic Line Forces.** The tether line forces are caused by the elasticity of the tether material and are directed parallel to the cable line. Tether line flexibility generates resistive stiffness and damping forces proportional to cable line extension and extension rate. Using the bead position and velocity matrices, tether line element vectors can be formed.

$$\Delta_T = R_T([1 : N_B + 1], :) - R_T([2 : N_B + 2], :), \text{ and} \quad (12)$$

$$\dot{\Delta}_T = \dot{R}_T([1 : N_B + 1], :) - \dot{R}_T([2 : N_B + 2], :). \quad (13)$$

The elastic tether line force, expressed in the inertial reference frame, is given by equation (14).

$$\begin{Bmatrix} X_{T_i} \\ Y_{T_i} \\ Z_{T_i} \end{Bmatrix} = \frac{F_{T_i}}{|\Delta_{T_i}|} \Delta_{T_i}^T. \quad (14)$$

The magnitude of the tether line force,  $F_{T_i}$ , is determined by equation (15).

$$F_{T_i} = \begin{cases} K_T (|\Delta_{T_i}| - L_{T_0}) + C_T \Delta V_{T_i}, & |\Delta_{T_i}| - L_{T_0} > 0 \\ 0, & |\Delta_{T_i}| - L_{T_0} \leq 0 \end{cases}. \quad (15)$$

The second condition in equation (15) stipulates that when the tether line is slack, no force is transmitted across the tether. As the tether stretches, the tether diameter decreases. The diameter reduction, as a function of tether line extension, can be computed using Poisson's ratio for the tether material.

$$D_{T_i} = D_T \left(1 - v_T \frac{L_{T_i} - L_{T_0}}{L_{T_0}}\right). \quad (16)$$

**3.2 Aerodynamic Line Forces.** Aerodynamic forces on the tether line are generated by two sources: skin friction and flat plate drag. The matrices  $P_T$  and  $\dot{P}_T$ , defined by equations (17) and (18), are used to compute tether aerodynamic forces.

$$P_T = \frac{1}{2} (\Delta_T ([1: N_B + 1], :) + \Delta_T ([2: N_B + 2], :)), \text{ and} \quad (17)$$

$$\dot{P}_T = \frac{1}{2} (\dot{\Delta}_T ([1: N_B + 1], :) + \dot{\Delta}_T ([2: N_B + 2], :)). \quad (18)$$

Skin friction drag acts in a direction parallel to the tether line and is given by equation (19).

$$D_{SF_i} = -\frac{1}{2} \rho_i v_{SF_i} |v_{SF_i}| \frac{\tilde{L}_{T_i}}{2} \pi \tilde{D}_{T_i} C_{SF}. \quad (19)$$

Aerodynamic loads on a particular tether bead are obtained using average tether bead direction, diameter, and length from adjacent line elements. The skin friction drag coefficient is a function of the local Mach number at the tether bead. In the inertial reference frame, the skin friction drag exerted on a tether bead is given by equation (20).

$$\begin{Bmatrix} X_{SF_i} \\ Y_{SF_i} \\ Z_{SF_i} \end{Bmatrix} = \frac{D_{SF_i}}{|P_{T_i}|} P_{T_i}^T. \quad (20)$$

The local aerodynamic velocity along a tether bead element,  $v_{SF_i}$ , can be computed by a dot product of the velocity vector with the normalized tether bead direction vector.

$$v_{SF_i} = \frac{\dot{R}_{T_i} \bullet P_{T_i}}{|P_{T_i}|}. \quad (21)$$

The flat plate drag force exerted on the tether line element responds normally to the tether bead element vector and is directed parallel to the aerodynamic velocity normal to the tether bead direction vector.

$$D_{FP_i} = -\frac{1}{2} \rho_i (v_{FP_i} \bullet v_{FP_i}) \tilde{L}_{T_i} \tilde{D}_{T_i} C_{FP}. \quad (22)$$

The flat plate velocity vector is computed by subtracting the skin friction drag velocity from the total tether bead inertial velocity.

$$v_{FP_i} = \begin{Bmatrix} \dot{x}_{T_i} \\ \dot{y}_{T_i} \\ \dot{z}_{T_i} \end{Bmatrix} - \frac{(\dot{R}_{T_i} \bullet P_{T_i}) P_{T_i}^T}{|P_{T_i}|^2}. \quad (23)$$

The flat plate drag coefficient,  $C_{FP}$ , is a function of the Mach number at the tether bead. The flat plate drag force expressed in the inertial reference frame is given by equation (24).

$$\begin{Bmatrix} X_{FP_i} \\ Y_{FP_i} \\ Z_{FP_i} \end{Bmatrix} = \frac{D_{FP_i}}{|v_{FP_i}|} v_{FP_i}^T. \quad (24)$$

## 4. Reel Dynamic Model

The tether reel is assumed to consist of a rotating reel acted on by an elastic line force,  $F_E$ , that tends to pay out the tether line and a resistance force,  $F_R$ , which opposes the unreeling process. Rather than using reel rotation as a degree of freedom, it is more convenient to use

tether line pay-out as a dynamic variable. Equation (25) governs the dynamics of the tether line unreeling process.

$$m_R \ddot{s}_R + c_R \dot{s}_R + k_R s_R = F_E. \quad (25)$$

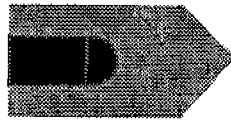
The tether reel damping and stiffness coefficients are scheduled as a function of tether pay-out so that the unreeling process can be dynamically tailored. The tether pay-out dynamic equation is a linear second order system with variable coefficients. With this general equation, any reel geometry that exhibits second order behavior can be accommodated.

## 5. Flight Phases

Simulation of the complete mission involves four distinct flight phases. When initially deployed from an aircraft, both projectiles are rigidly connected so the complete system moves as a rigid body. At a specific time after munition release, the follower projectile is unrestrained from the lead projectile and the tether line commences its unreeling process. The third flight phase is the time between when the tether line is completely unreeled and when the lead projectile impacts the target. After the lead projectile hits the target and stops moving, the follower projectile and the tether line continue their motion toward the target. A cartoon of the first four flight phases is provided in Figure 2.

## 6. Results

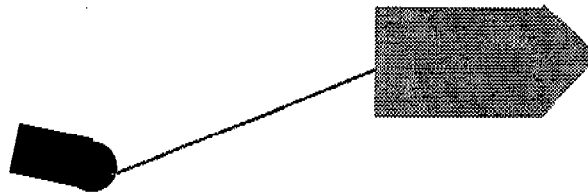
In order to exercise the dynamic model previously described, simulation results for an example system are shown. The baseline lead projectile is a 2,000 lb, fin-stabilized projectile. The tether line is 1,000 ft long with a total weight of approximately 3 lb. The reel stiffness coefficient is 0.1, and the reel damping is 1.0. It is assumed that the lead projectile is



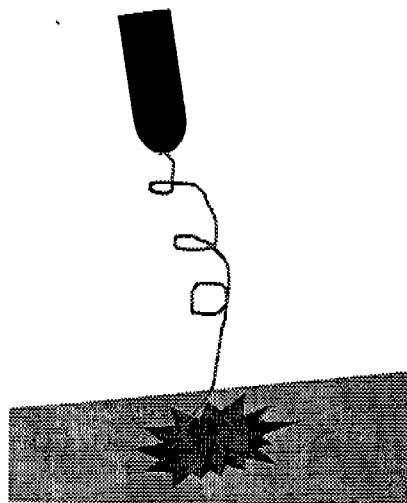
**(a) Initial Configuration**



**(b) Deployment Configuration**



**(c) Fully Deployed Configuration**



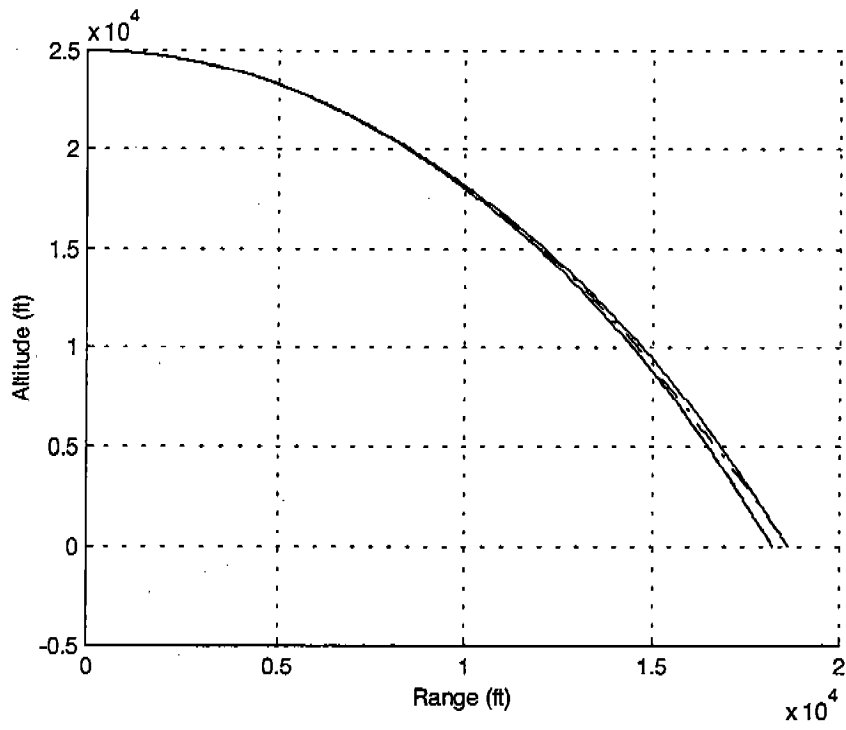
**(d) Terminal Configuration**

**Figure 2. Deployment Schematic.**

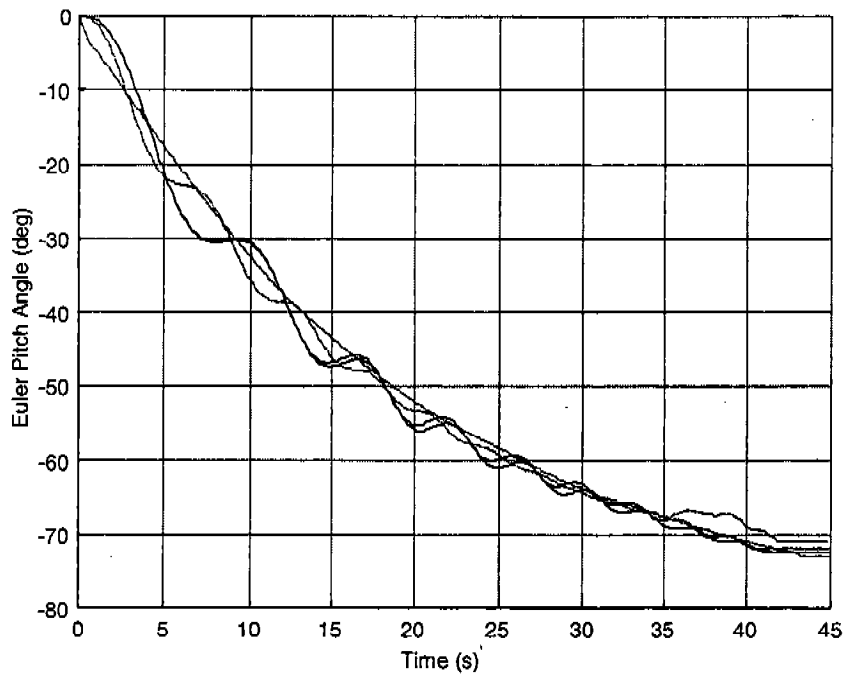
mounted on the parent aircraft such that the body axes of the aircraft and the lead projectile are aligned. The lead projectile is deployed from the parent aircraft that is flying straight and level at a speed of 500 ft/s. The effect of munition release on the lead projectile is to impart an initial vertical velocity of 10 ft/s downward on the lead projectile. All other initial conditions are zero. The lead and follower projectiles are separated at  $T = 0$  s.

Figure 3 plots the range of the lead and follower projectiles for a follower-to-lead mass ratio of 1% and 100%. The 100% mass ratio case has a slightly greater range because the projectiles separate more slowly and reel resistance is reduced. For a given mass ratio, both the lead and follower projectiles follow similar trajectories. The total flight time is approximately 40 s. Figures 4 and 6 show the pitch attitude and pitch rate for the same conditions as Figure 3. The pitch angle of both projectiles follows the same trends of decreasing from a level attitude to below  $70^\circ$  nose down at impact. The lead projectile oscillates at a frequency of  $1/7$  cycles per second. Figure 5 shows the forward body velocity of the lead and follower projectiles for a mass ratio of 1% and 100%. The lowest trace with oscillations at  $T = 22$  s is the follower projectile for a mass ratio of 1%. The lead projectile is the middle trace at  $T = 30$  s. The lead projectile tends to increase in speed more than the follower projectile. The follower projectile does not slow down because as the tether line pays out, the resistance force in the tether reel tends to pull the follower projectile with the lead projectile. At about 22 s into flight, the tether line is fully deployed, and the lead projectile “snatches” the follower projectile and sharply increases its speed. The elastic nature of the tether line increases the speed of the follower projectile such that it is greater than the lead projectile.

At the first peak in the follower projectile velocity time trace, the tether line goes slack and no force is transmitted along the tether line. At this point, the follower projectile is essentially uncoupled from both the lead projectile and the tether line. For this reason, the follower projectile begins to slow down to its uncoupled steady state drop velocity. The follower projectile continues to slow down until approximately 22.7 s into flight, when the lead projectile “snatches” the follower projectile again and rapidly increases its speed. This sequence continues



**Figure 3. Range (Mass Ratio = 1%, 100%).**



**Figure 4. Pitch Angle (Lead Follower, Mass Ratio = 1%, 100%).**

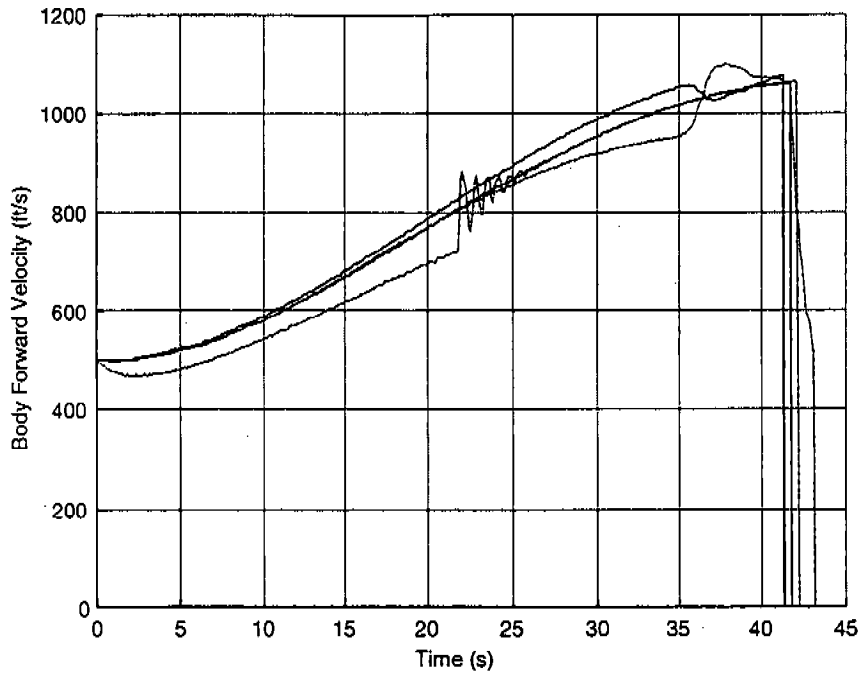


**Figure 5. Body Forward Velocity (Lead/Follower, Mass Ratio = 1%, 100%).**

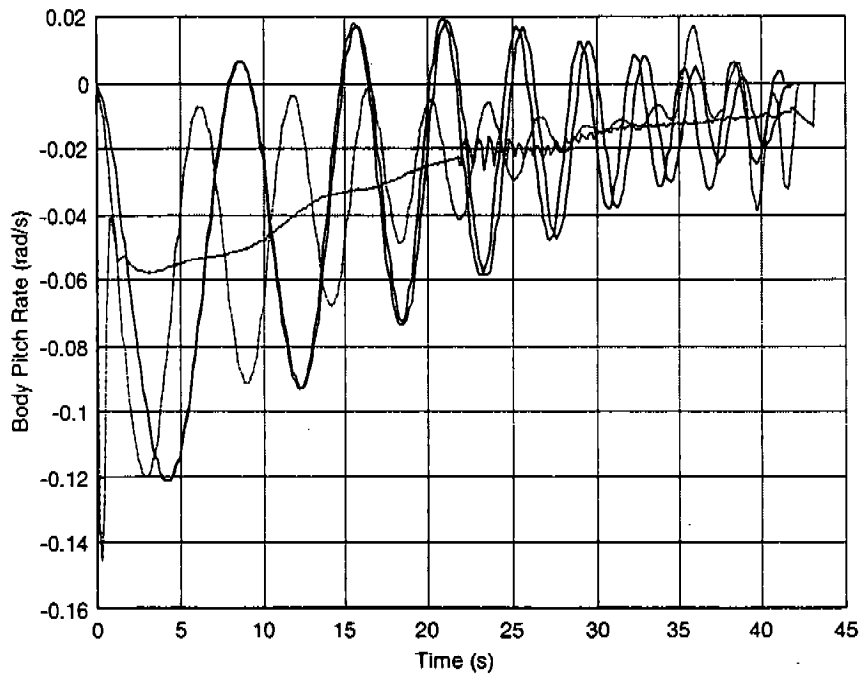


**Figure 6. Pitch Rate (Lead/Follower, Mass Ratio = 1%, 100%).**

for six cycles, and then the lead and follower projectiles enter a steady state condition. At  $t = 42$  s, the lead projectile impacts the ground and obviously stops moving. The tether line rapidly goes slack and again the follower projectile speed slows as it seeks to attain steady state drop velocity. Notice for this mass ratio, the lead projectile is essentially unaffected by the follower projectile and the tether. At  $T = 30$  s, the lower trace is the follower projectile, and the upper trace is the lead projectile for a mass ratio of 100%. Notice for this mass ratio, the line takes longer to deploy due to the similar dynamic characteristics of both bodies, and significant interaction between the lead and follower projectiles exists. The plot representing the angle of attack vs. time (Figure 7) shows that the angle of attack remains small for both the lead and follower projectiles.

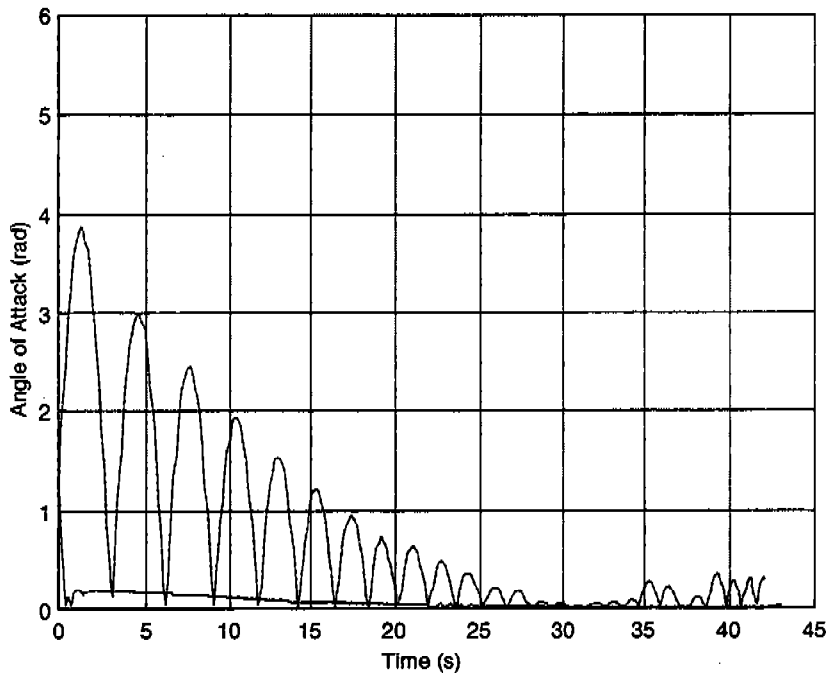


**Figure 7. Angle of Attack (Lead/Follower, Mass Ratio = 1%, 100%).**

For a mass ratio of 100%, Figures 8–12 show parametric trends on the response of the system to different drag coefficient ratios between the lead and follower projectiles. The range and pitch attitude characteristics are similar for all drag ratios considered. However, the lead and follower forward velocity time histories show a predictable speed reduction as the drag ratio is increased

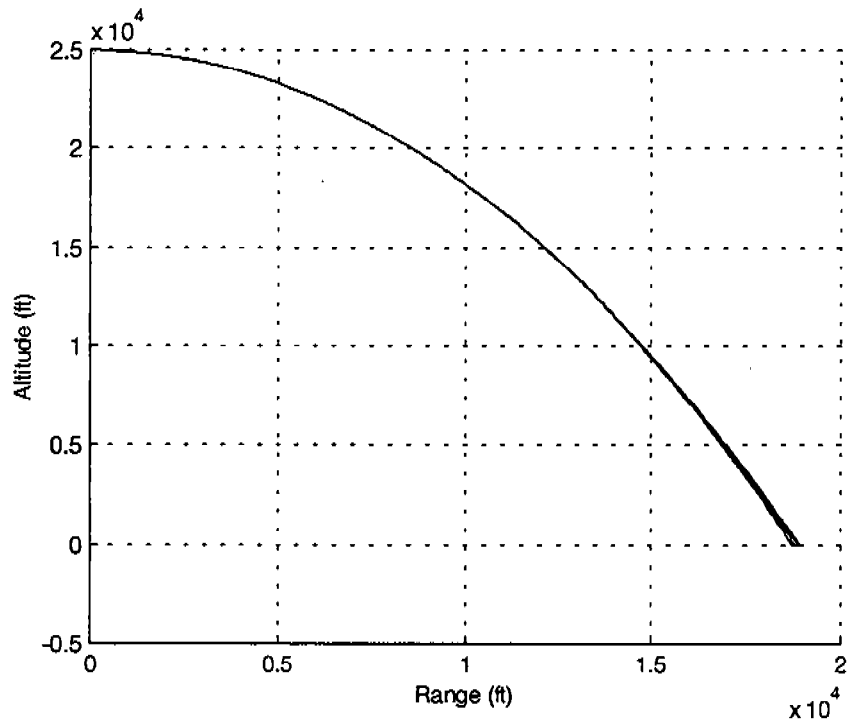


Figure 8. Range (Lead/Follower, Mass Ratio = 100%, Drag Coefficient Ratio = 1.25, 1.5, 1.75, 2).

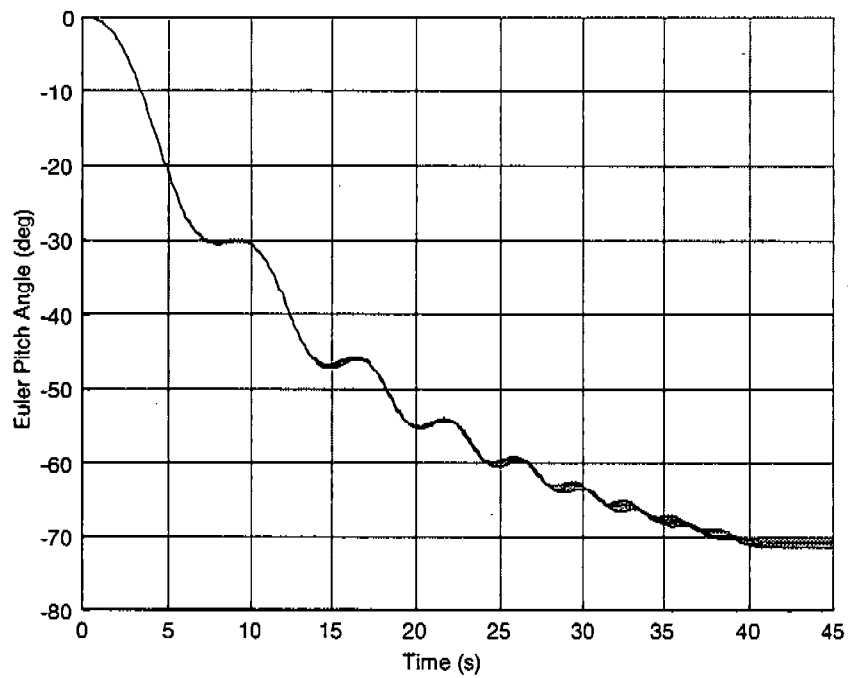


Figure 9. Pitch Angle (Lead/Follower, Mass Ratio = 100%, Drag Coefficient Ratio = 1.25, 1.5, 1.75, 2).

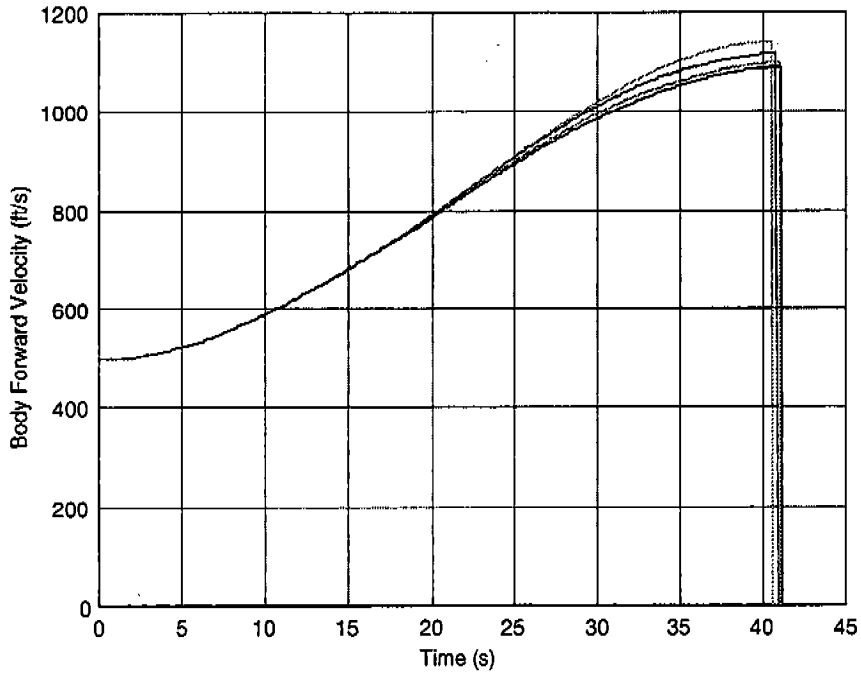


Figure 10. Lead Forward Velocity (Mass Ratio = 100%, Drag Coefficient Ratio = 1.25, 1.5, 1.75, 2).

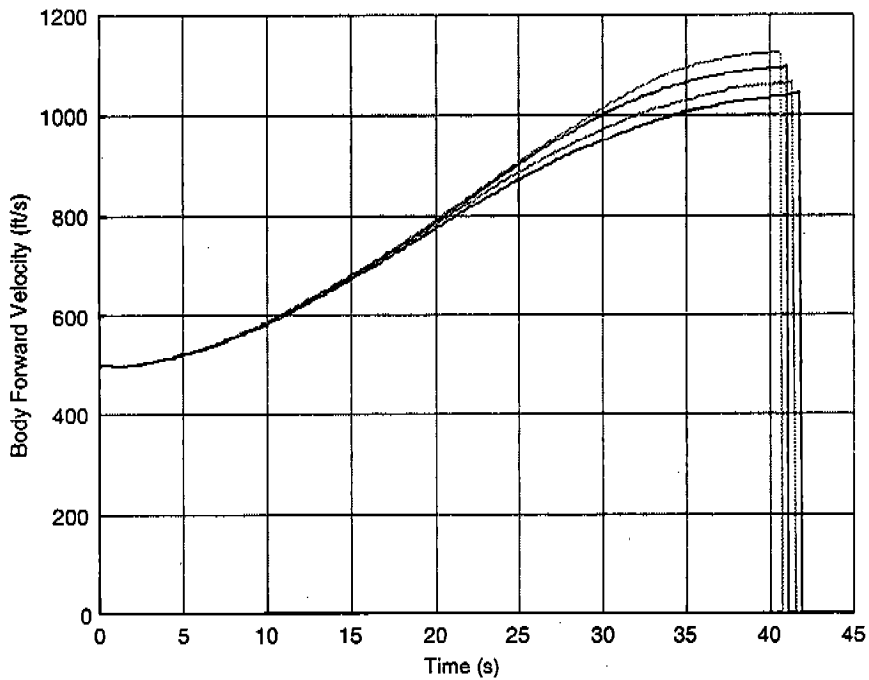
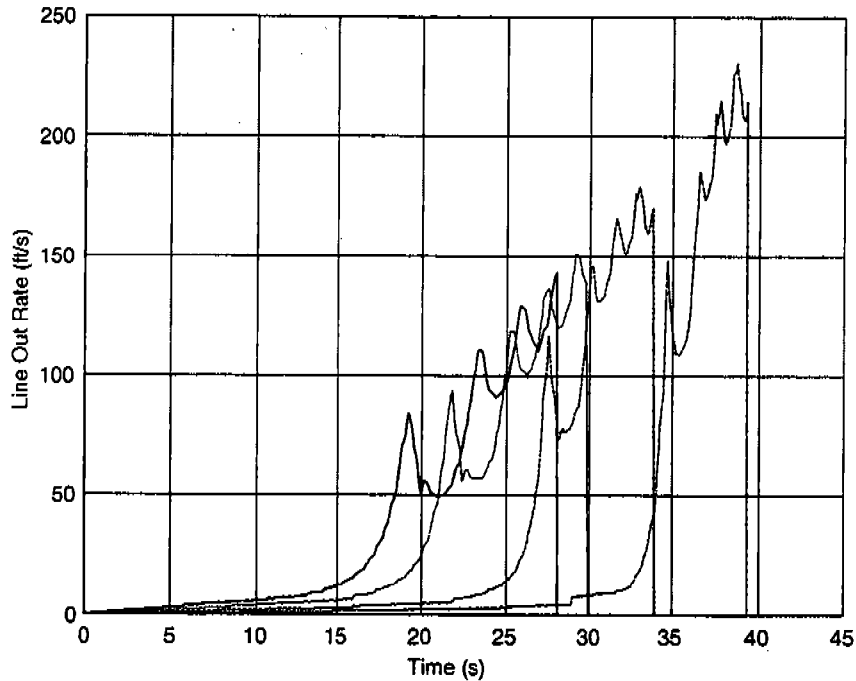


Figure 11. Follower Forward Velocity (Mass Ratio = 100%, Drag Coefficient Ratio = 1.25, 1.5, 1.75, 2).



**Figure 12. Tether Line Out Rate (Mass Ratio = 100%, Drag Coefficient Ratio = 1.25, 1.5, 1.75, 2).**

because higher drag ratios pay out the line more rapidly and increase the lead projectile resistance.

For a mass ratio of 1%, Figures 13–19 show parametric trends on the response of the system to different drag coefficient ratios between the lead and follower projectiles. As in the previous case, the lead and follower forward velocity time histories show a predictable speed reduction as the drag ratio is increased. However, the basic shape of the curve shows an oscillation induced by the snatch load.

## 7. Conclusions

A dynamic model has been developed for the flight mechanics of two projectiles connected by a flexible tether. Both projectiles are individually modeled with six degrees of freedom. The projectile aerodynamic model depends on the attack angle and Mach number, and includes high

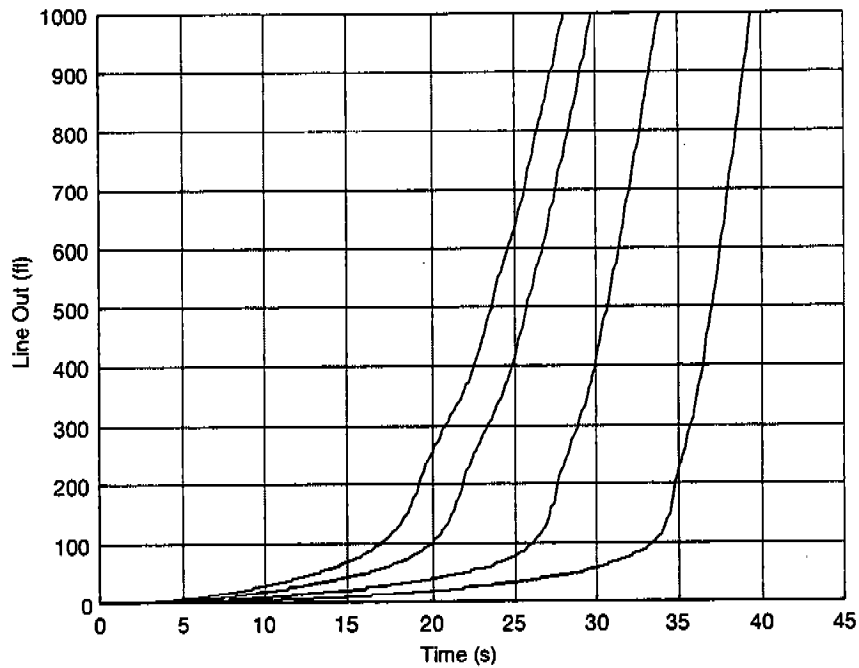


Figure 13. Tether Line Out (Mass Ratio = 100%, Drag Coefficient Ratio = 1.25, 1.5, 1.75, 2).

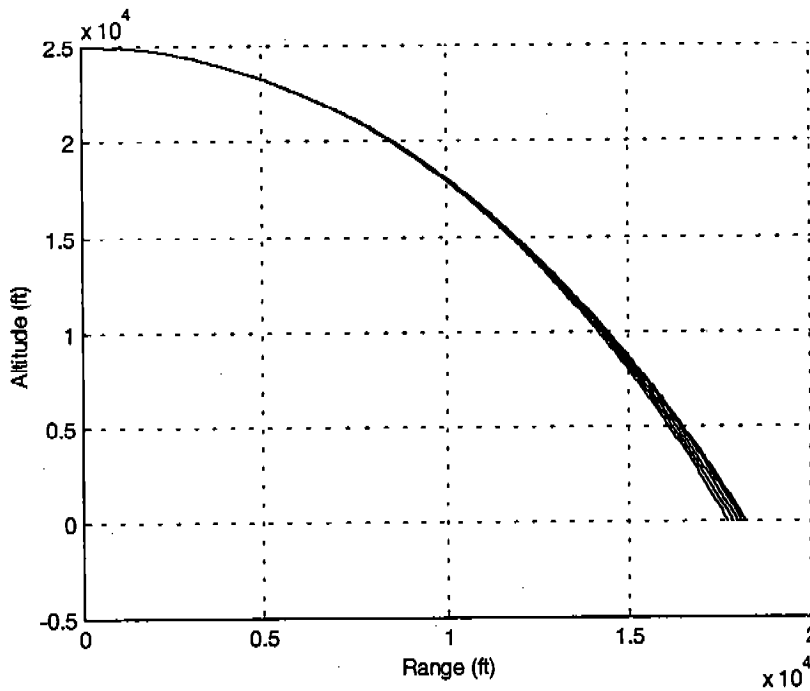
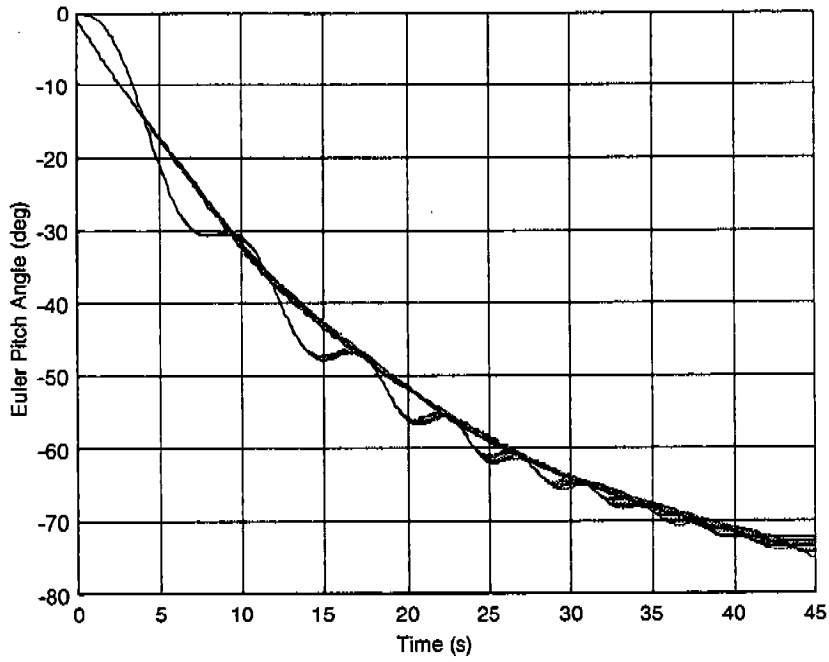
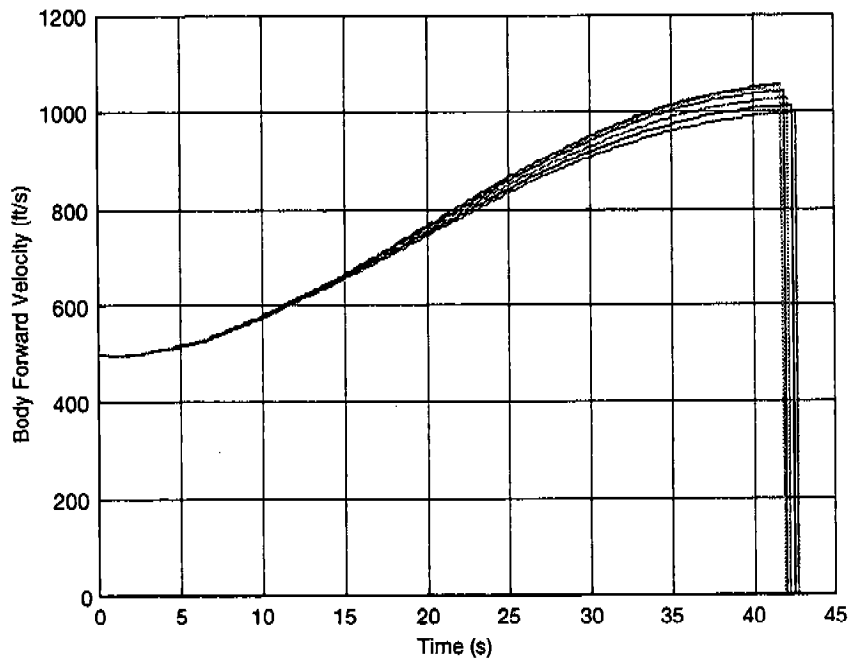


Figure 14. Range (Mass Ratio = 1%, Drag Coefficient Ratio = 1.0625, 1.125, 1.25, 1.5, 1.75, 2).



**Figure 15. Pitch Angle (Lead/Follower, Mass Ratio = 1%, Drag Coefficient Ratio = 1.0625, 1.125, 1.25, 1.5, 1.75, 2).**



**Figure 16. Lead Forward Velocity (Mass Ratio = 1%, Drag Coefficient Ratio = 1.0625, 1.125, 1.25, 1.5, 1.75, 2).**

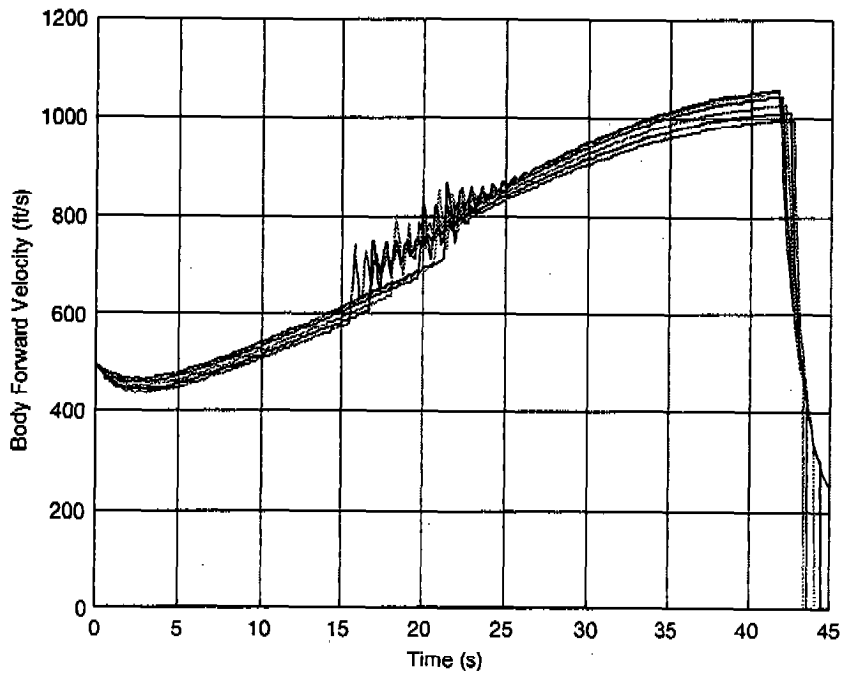


**Figure 17. Follower Forward Velocity (Mass Ratio = 1%, Drag Coefficient Ratio = 1.0625, 1.125, 1.25, 1.5, 1.75, 2).**

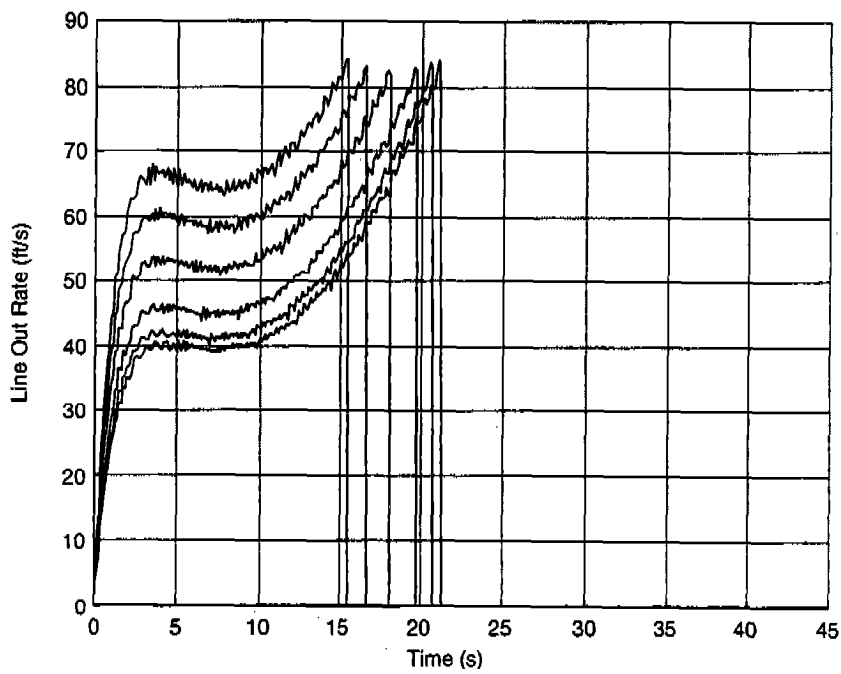


**Figure 18. Tether Line Out Rate (Mass Ratio = 1%, Drag Coefficient Ratio = 1.0625, 1.125, 1.25, 1.5, 1.75, 2).**

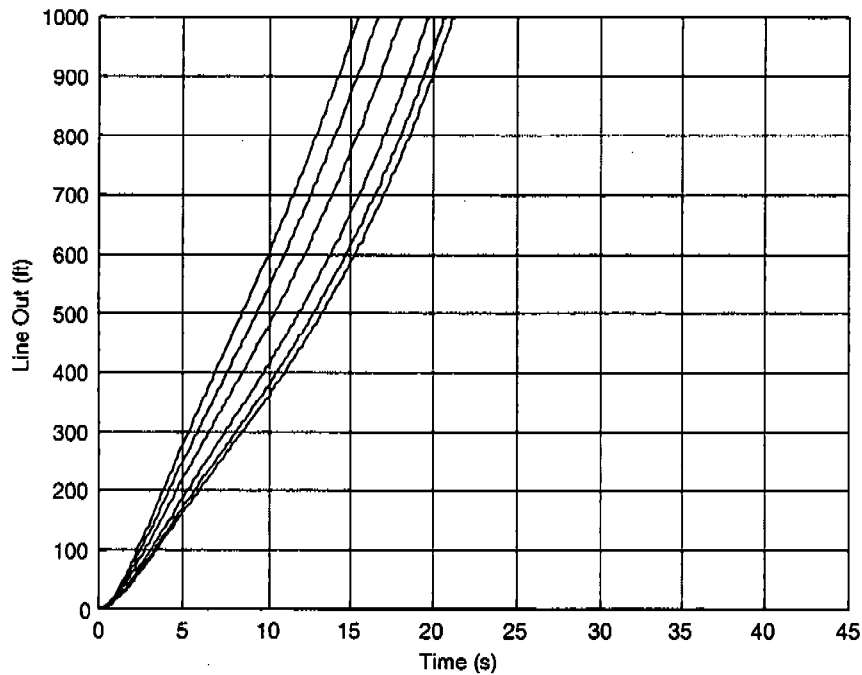


**Figure 19. Tether Line Out (Mass Ratio = 1%, Drag Coefficient Ratio = 1.0625, 1.125, 1.25, 1.5, 1.75, 2).**

angle of attack terms as well as unsteady roll, pitch, and yaw aerodynamic damping. The tether is split into a finite number of beads, with each bead containing three translational degrees of freedom. Forces acting on the beads include weight, line stiffness, line damping, and aerodynamic drag. The tether aerodynamic drag force is dependent on the tether line angle of attack and Mach number. The tether line pay-out process is modeled with a single degree of freedom and allows for a resistive damping and stiffness force to resist tether line pay out. For follower projectiles relatively low in weight, the lead projectile motion is uncoupled. An oscillation in the forward velocity of the follower projectile is induced at the point where the tether line is completely deployed. However, for lead and follower projectile configurations with similar mass, lead projectile motion is coupled to the tether and follower projectile.

INTENTIONALLY LEFT BLANK.

## 8. References

1. Tye, G., and R. Han. "Attitude Dynamics Investigation of the OEDIPUS – A Tethered Rocket Payload." *Journal of Spacecraft and Rockets*, vol. 32, no. 1, 1995.
2. Puig-Suari, J., J. Longuski, and S. Tragesser. "Aerocapture With a Flexible Tether." *Journal of Guidance, Control, and Dynamics*, vol. 18, no. 6, 1995.
3. No, T. S., and J. E. Cochran. "Dynamics and Control of a Tethered Flight Vehicle." *Journal of Guidance, Control, and Dynamics*, vol. 18, no. 1, 1995.
4. Phillips, W. H. "Theoretical Analysis of Oscillations of a Towed Cable." NACA Technical Note 1796, National Advisory Committee for Aeronautics, Langley Aeronautical Laboratory, VA, 1949.
5. Clifton, J. M., L. V. Schmidt, and T. D. Stuart. "Dynamic Modeling of a Trailing Wire Towed by an Orbiting Aircraft." *Journal of Guidance, Control, and Dynamics*, vol. 18, no. 4, 1995.
6. Djerassi, S., and V. Viderman. "Motion Analysis of Two, Cable Connected Bodies in Atmospheric Free Fall." *Proceedings of the 1997 AIAA Atmospheric Flight Mechanics Conference*, New Orleans, LA, 1997.
7. Costello, M. F., and D. A. Anderson. "Effect of Internal Mass Unbalance on the Stability and Terminal Accuracy of a Field Artillery Projectile." *Proceedings of the 1996 AIAA Atmospheric Flight Mechanics Conference*, San Diego, CA, 1996.
8. Etkin, B. *Dynamics of Atmospheric Flight*. New York: John Wiley and Sons, 1972.
9. Murphy, C. *Free Flight of Symmetric Missiles*. Ballistics Research Laboratory Report BRL-1216, U.S. Army Ballistics Research Laboratory, Aberdeen Proving Ground, MD, 1963.
10. Von Mises, R. *Theory of Flight*. New York: Dover Publications Inc., 1959.

INTENTIONALLY LEFT BLANK.

## List of Symbols

$x_L, y_L, z_L$	Components of the center-of-mass position vector of the lead projectile expressed in the inertial reference frame
$x_F, y_F, z_F$	Components of the center-of-mass position vector of the follower projectile expressed in the inertial reference frame
$x_{T_i}, y_{T_i}, z_{T_i}$	Components of the inertial position vector of the $i$ th tether bead
$\phi_L, \theta_L, \psi_L$	Euler roll, pitch, and yaw angles of the lead projectile
$\phi_F, \theta_F, \psi_F$	Euler roll, pitch, and yaw angles of the follower projectile
$u_L, v_L, w_L$	Translation velocity components of the center of mass of the lead projectile resolved in the lead projectile body reference frame
$u_F, v_F, w_F$	Translation velocity components of the center-of-mass of the follower projectile resolved in the follower projectile body reference frame
$p_L, q_L, r_L$	Components of the angular velocity vector of the lead projectile expressed in the lead projectile body reference frame
$p_F, q_F, r_F$	Components of the angular velocity vector of the follower projectile expressed in the follower projectile body reference frame
$X_L, Y_L, Z_L$	External forces on the lead projectile expressed in the lead projectile body axes
$X_F, Y_F, Z_F$	External forces on the follower projectile expressed in the follower projectile body axes
$L_L, M_L, N_L$	External moments on the lead projectile expressed in the lead projectile body axes
$L_F, M_F, N_F$	External moments on the follower projectile expressed in the follower projectile body axes
$m_L$	Lead projectile mass
$m_F$	Follower projectile mass
$[I_L]$	Mass moment of inertia matrix of the lead projectile
$[I_F]$	Mass moment of inertia matrix of the follower projectile
$D_L$	Lead projectile characteristic length (diameter)
$C_i^L$	Lead projectile aerodynamic coefficients
$m_{T_i}, W_{T_i}$	Mass and weight of $i$ th tether bead
$K_T$	Tether line stiffness
$C_T$	Tether line damping
$\rho_i$	Local air density of a tether line element
$\tilde{L}_{T_i}$	Average length of adjacent tether line elements
$\tilde{D}_{T_i}$	Average diameter of adjacent tether line elements

$v_{SF_i}$	Local aerodynamic velocity in the direction of a tether bead
$C_{SF}$	Skin friction drag coefficient of the tether line
$C_{FP}$	Flat plate drag coefficient of the tether line
$s_R$	Tether line pay-out length
$m_R$	Tether reel mass
$\nu_T$	Poisson's ratio of the tether line material

<u>NO. OF COPIES</u>	<u>ORGANIZATION</u>	<u>NO. OF COPIES</u>	<u>ORGANIZATION</u>
2	DEFENSE TECHNICAL INFORMATION CENTER DTIC DDA 8725 JOHN J KINGMAN RD STE 0944 FT BELVOIR VA 22060-6218	1	DIRECTOR US ARMY RESEARCH LAB AMSRL D D R SMITH 2800 POWDER MILL RD ADELPHI MD 20783-1197
1	HQDA DAMO FDT 400 ARMY PENTAGON WASHINGTON DC 20310-0460	1	DIRECTOR US ARMY RESEARCH LAB AMSRL DD 2800 POWDER MILL RD ADELPHI MD 20783-1197
1	OSD OUSD(A&T)/ODDDR&E(R) R J TREW THE PENTAGON WASHINGTON DC 20301-7100	1	DIRECTOR US ARMY RESEARCH LAB AMSRL CS AS (RECORDS MGMT) 2800 POWDER MILL RD ADELPHI MD 20783-1145
1	DPTY CG FOR RDA US ARMY MATERIEL CMD AMCRDA 5001 EISENHOWER AVE ALEXANDRIA VA 22333-0001	3	DIRECTOR US ARMY RESEARCH LAB AMSRL CI LL 2800 POWDER MILL RD ADELPHI MD 20783-1145
1	INST FOR ADVNCD TCHNLGY THE UNIV OF TEXAS AT AUSTIN PO BOX 202797 AUSTIN TX 78720-2797		<u>ABERDEEN PROVING GROUND</u>
1	DARPA B KASPAR 3701 N FAIRFAX DR ARLINGTON VA 22203-1714	4	DIR USARL AMSRL CI LP (BLDG 305)
1	NAVAL SURFACE WARFARE CTR CODE B07 J PENNELLA 17320 DAHLGREN RD BLDG 1470 RM 1101 DAHLGREN VA 22448-5100		
1	US MILITARY ACADEMY MATH SCI CTR OF EXCELLENCE DEPT OF MATHEMATICAL SCI MADN MATH THAYER HALL WEST POINT NY 10996-1786		

<u>NO. OF COPIES</u>	<u>ORGANIZATION</u>
3	AIR FORCE RSRCH LAB MUNITIONS DIR AFRL/MNAV G ABATE 101 W EGLIN BLVD STE 219 EGLIN AFB FL 32542
3	ALLEN PETERSON 159 S HIGHLAND DR KENNEWICK WA 99337
1	CDR WL/MNMF D MABRY 101 W EGLIN BLVD STE 219 EGLIN AFB FL 32542-6810
20	DEPT OF MECHL ENGRG M COSTELLO OREGON STATE UNIVERSITY CORVALLIS OR 97331
4	CDR US ARMY ARDEC AMSTA AR CCH J DELORENZO S MUSALI R SAYER P DONADIO PICATINNY ARESENAL NJ 07806-5000
7	CDR US ARMY TANK MAIN ARMAMENT SYSTEM AMCPM TMA D GUZIEWICZ R DARCEY C KIMKER R JOINSON E KOPOAC T LOUZIERIO C LEVECHIA PICATINNY ARESENAL NJ 07806-5000
1	CDR USA YUMA PROV GRND STEYT MTW YUMA AZ 85365-9103

<u>NO. OF COPIES</u>	<u>ORGANIZATION</u>
10	CDR US ARMY TACOM AMCPEO HFM AMCPEO HFM F AMCPEO HFM C AMCPM ABMS AMCPM BLOCKIII AMSTA CF AMSTA Z AMSTA ZD AMCPM ABMS S W DR PATTISON A HAVERILLA WARREN MI 48397-5000
1	DIR BENET LABORATORIES SMCWV QAR T MCCLOSKEY WATERVLIET NY 12189-5000
1	CDR USAOTEA CSTE CCA DR RUSSELL ALEXANDRIA VA 22302-1458
2	DIR US ARMY ARMOR CTR & SCHL ATSB WP ORSA A POMEY ATSB CDC FT KNOX KY 40121
1	CDR US ARMY AMCCOM AMSMC ASR A MR CRAWFORD ROCK ISLAND IL 61299-6000
2	PROGRAM MANAGER GROUND WEAPONS MCRDAC LTC VARELA CBGT QUANTICO VA 22134-5000

<u>NO. OF COPIES</u>	<u>ORGANIZATION</u>
4	COMMANDER US ARMY TRADOC ATCD T ATCD TT ATTE ZC ATTG Y FT MONROE VA 23651-5000
1	NAWC F PICKETT CODE C2774 CLPL BLDG 1031 CHINA LAKE CA 93555
1	NAVAL ORDNANCE STATION ADVNC D SYS TCHNLGY BRNCH D HOLMES CODE 2011 LOUISVILLE KY 40214-5001
1	NAVAL SURFACE WARFARE CTR F G MOORE DAHLGREN DIVISION CODE G04 DAHLGREN VA 22448-5000
1	US MILITARY ACADEMY MATH SCI CTR OF EXCELLENCE DEPT OF MATHEMATICAL SCI MDN A MAJ DON ENGEN THAYER HALL WEST POINT NY 10996-1786
3	DIR SNL A HODAPP W OBERKAMPF F BLOTTNER DIVISION 1631 ALBUQUERQUE NM 87185
3	ALLIANT TECH SYSTEMS C CANDLAND R BURETTA R BECKER 7225 NORTHLAND DR BROOKLYN PARK MN 55428

<u>NO. OF COPIES</u>	<u>ORGANIZATION</u>
3	DIR USARL AMSRL SE RM H WALLACE AMSRL SS SM J EIKE A LADAS 2800 POWDER MILL RD ADELPHI MD 20783-1145
1	OFC OF ASST SECY OF ARMY FOR R&D SARD TR W MORRISON 2115 JEFFERSON DAVIS HWY ARLINGTON VA 22202-3911
2	CDR USARDEC AMSTA FSP A S DEFEO R SICIGNANO PICATINNY ARESENAL NJ 07806-5000
2	CDR USARDEC AMSTA AR CCH A M PALATHINGAL R CARR PICATINNY ARESENAL NJ 07806-5000
5	TACOM ARDEC AMSTA AR FSA K CHIEFA AMSTA AR FS A WARNASCH AMSTA AR FSF W RYBA AMSTA AR FSP S PEARCY J HEDDERICH PICATINNY ARESENAL NJ 07806-5000

<u>NO. OF COPIES</u>	<u>ORGANIZATION</u>
5	CDR US ARMY MICOM AMSMI RD P JACOBS P RUFFIN AMSMI RD MG GA C LEWIS AMSMI RD MG NC C ROBERTS AMSMI RD ST GD D DAVIS RSA AL 35898-5247
3	CDR US ARMY AVN TRP CMD DIRECTORATE FOR ENGINEERING AMSATR ESW M MAMOUD M JOHNSON J OBERMARK RSA AL 35898-5247
1	DIR US ARMY RTTC STERT TE F TD R EPPS BLDG 7855 REDSTONE ARSENAL AL 38598-8052
2	STRICOM AMFTI EL D SCHNEIDER R COLANGELO 12350 RESEARCH PKWY ORLANDO FL 32826-3276
1	CDR OFFICE OF NAVAL RES CODE 333 J GOLDWASSER 800 N QUINCY ST RM 507 ARLINGTON VA 22217-5660
1	CDR US ARMY RES OFFICE AMXRO RT IP TECH LIB PO BOX 12211 RESEARCH TRIANGLE PARK NJ 27709-2211

<u>NO. OF COPIES</u>	<u>ORGANIZATION</u>
4	CDR US ARMY AVN TRP CMD AVIATION APPLIED TECH DIR AMSATR TI R BARLOW E BERCHER T CONDON B TENNEY FT EUSTIS VA 23604-5577
3	CDR NAWC WEAPONS DIV CODE 543400D S MEYERS CODE C2744 T MUNSINGER CODE C3904 D SCOFIELD CHINA LAKE CA 93555-6100
1	CDR NSWC CRANE DIVISION CODE 4024 J SKOMP 300 HIGHWAY 361 CRANE IN 47522-5000
1	CDR NSWC DAHLGREN DIV CODE 40D J BLANKENSHIP 6703 WEST HWY 98 PANAMA CITY FL 32407-7001
1	CDR NSWC J FRAYSEE D HAGEN 17320 DAHLGREN RD DAHLGREN VA 22448-5000

<u>NO. OF COPIES</u>	<u>ORGANIZATION</u>
5	CDR NSWC INDIAN HEAD DIV CODE 40D D GARVICK CODE 4110C L FAN CODE 4120 V CARLSON CODE 4140E H LAST CODE 450D T GRIFFIN 101 STRAUSS AVE INDIAN HEAD MD 20640-5000
1	CDR NSWC INDIAN HEAD DIV LIBRARY CODE 8530 BLDG 299 101 STRAUSS AVE INDIAN HEAD MD 20640
2	US MILITARY ACADEMY MATH SCI CTR OF EXCELLENCE DEPT OF MATHEMATICAL SCI MDN A MAJ D ENGEN R MARCHAND THAYER HALL WEST POINT NY 10996-1786
3	CDR US ARMY YUMA PG STEYP MT AT A A HOOPER STEYP MT EA YUMA AZ 85365-9110
6	CDR NSWC INDIAN HEAD DIV CODE 570D J BOKSER CODE 5710 L EAGLES J FERSUSON CODE 57 C PARIS CODE 5710G S KIM CODE 5710E S JAGO 101 STRAUSS AVE ELY BLDG INDIAN HEAD MD 20640-5035

<u>NO. OF COPIES</u>	<u>ORGANIZATION</u>
1	BRUCE KIM MICHIGAN STATE UNIVERSITY 2120 ENGINEERING BLDG EAST LANSING MI 48824-1226
2	INDUSTRIAL OPERATION CMD AMFIO PM RO W MCKELVIN MAJ BATEMAN ROCK ISLAND IL 61299-6000
3	PROGRAM EXECUTIVE OFFICER TACTICAL AIRCRAFT PROGRAMS PMA 242 1 MAJ KIRBY R242 PMA 242 33 R KEISER (2 CPS) 1421 JEFFERSON DAVIS HWY ARLINGTON VA 22243-1276
1	CDR NAVAL AIR SYSTEMS CMD CODE AIR 471 A NAKAS 1421 JEFFERSON DAVIS HWY ARLINGTON VA 22243-1276
4	ARROW TECH ASSOCIATES INC R WHYTE A HATHAWAY H STEINHOFF 1233 SHELBOURNE RD SUITE D8 SOUTH BURLINGTON VT 05403
3	US ARMY AVIATION CTR DIR OF COMBAT DEVELOPMENT ATZQ CDM C B NELSON ATZQ CDC C T HUNDLEY ATZQ CD G HARRISON FORT RUCKER AL 36362

NO. OF  
COPIES ORGANIZATION

NO. OF  
COPIES ORGANIZATION

ABERDEEN PROVING GROUND

ABERDEEN PROVING GROUND (CONTD)

3 CDR  
USA ARDEC  
AMSTA AR FSF T  
R LIESKE  
J WHITESIDE  
J MATTS  
BLDG 120

1 CDR  
USA TECOM  
AMSTE CT  
T J SCHNELL  
RYAN BLDG

3 CDR  
USA AMSAA  
AMXSY EV  
G CASTLEBURY  
R MIRABELLE  
AMXSY EF  
S MCKEY

58 DIR USARL  
AMSRL WM  
I MAY  
T ROSENBERGER  
AMSRL WM BA  
W HORST JR  
W CIEPELLA  
AMSRL WM BE  
M SCHMIDT  
AMSRL WM BA  
F BRANDON  
T BROWN (5 CPS)  
L BURKE  
J CONDON  
B DAVIS  
T HARKINS (5 CPS)  
D HEPNER  
V LEITZKE  
M HOLLIS  
A THOMPSON

AMSRL WM BB  
B HAUG  
AMSRL WM BC  
J GARNER  
AMSRL WM BD  
B FORCH  
AMSRL WM BF  
J LACETERA  
P HILL  
AMSRL WM BR  
C SHOEMAKER  
J BORNSTEIN  
AMSRL WM BA  
G BROWN  
B DAVIS  
T HARKINS  
D HEPNER  
A THOMPSON  
J CONDON  
W DAMICO  
F BRANDON  
AMSRL WM BC  
P PLOSTINS (4 CPS)  
G COOPER  
B GUIDOS  
J SAHU  
M BUNDY  
K SOENCKSEN  
D LYON  
A HORST  
I MAY  
J BENDER  
J NEWILL  
AMSRL WM BC  
V OSKAY  
S WILKERSON  
W DRYSDALE  
R COATES  
A MIKHAL  
J WALL

# REPORT DOCUMENTATION PAGE

Form Approved  
OMB No. 0704-0188

Public reporting burden for this collection of information is estimated to average 1 hour per response, including the time for reviewing instructions, searching existing data sources, gathering and maintaining the data needed, and completing and reviewing the collection of information. Send comments regarding this burden estimate or any other aspect of this collection of information, including suggestions for reducing this burden, to Washington Headquarters Services, Directorate for Information Operations and Reports, 1215 Jefferson Davis Highway, Suite 1204, Arlington, VA 22202-4302, and to the Office of Management and Budget, Paperwork Reduction Project (0704-0188), Washington, DC 20503.

1. AGENCY USE ONLY (Leave blank)		2. REPORT DATE July 2000	3. REPORT TYPE AND DATES COVERED Final, Apr 98 - Apr 99	
4. TITLE AND SUBTITLE Simulation of Two Projectiles Connected by a Flexible Tether			5. FUNDING NUMBERS AH80	
6. AUTHOR(S) Mark F. Costello* and Geoffrey W. Frost*				
7. PERFORMING ORGANIZATION NAME(S) AND ADDRESS(ES) Oregon State University Corvallis, OR 97331			8. PERFORMING ORGANIZATION REPORT NUMBER	
9. SPONSORING/MONITORING AGENCY NAMES(S) AND ADDRESS(ES) U.S. Army Research Laboratory ATTN: AMSRL-WM-BC Aberdeen Proving Ground, MD 21005-5066			10. SPONSORING/MONITORING AGENCY REPORT NUMBER ARL-CR-456	
11. SUPPLEMENTARY NOTES Oregon State University Corvallis, OR 97331				
12a. DISTRIBUTION/AVAILABILITY STATEMENT Approved for public release; distribution is unlimited.			12b. DISTRIBUTION CODE	
13. ABSTRACT (Maximum 200 words) <p>This report investigates the atmospheric flight mechanics of two projectiles connected by a flexible tether. Both projectiles are individually modeled with six degrees of freedom. The projectile aerodynamic model depends on angle of attack and Mach number and includes unsteady roll, pitch, and yaw aerodynamic damping. The tether is split into a finite number of beads, with each bead possessing three translation degrees of freedom. Forces acting on the beads include weight, line stiffness, line damping, and aerodynamic drag. The tether aerodynamic drag force is dependent on the tether line angle of attack and Mach number. The tether line deployment process is modeled with a single degree of freedom that permits unreeling resistance to be incorporated. The effect of follower-to-lead projectile mass ratio and drag coefficient ratio on system response are investigated.</p>				
14. SUBJECT TERMS smart munitions, projectile aerodynamics, projectile tether			15. NUMBER OF PAGES 38	
			16. PRICE CODE	
17. SECURITY CLASSIFICATION OF REPORT UNCLASSIFIED	18. SECURITY CLASSIFICATION OF THIS PAGE UNCLASSIFIED	19. SECURITY CLASSIFICATION OF ABSTRACT UNCLASSIFIED	20. LIMITATION OF ABSTRACT UL	

**INTENTIONALLY LEFT BLANK.**

USER EVALUATION SHEET/CHANGE OF ADDRESS

This Laboratory undertakes a continuing effort to improve the quality of the reports it publishes. Your comments/answers to the items/questions below will aid us in our efforts.

1. ARL Report Number/Author ARL-CR-456 (Costello) Date of Report July 2000

2. Date Report Received \_\_\_\_\_

3. Does this report satisfy a need? (Comment on purpose, related project, or other area of interest for which the report will be used.) \_\_\_\_\_

4. Specifically, how is the report being used? (Information source, design data, procedure, source of ideas, etc.) \_\_\_\_\_

5. Has the information in this report led to any quantitative savings as far as man-hours or dollars saved, operating costs avoided, or efficiencies achieved, etc? If so, please elaborate. \_\_\_\_\_

6. General Comments. What do you think should be changed to improve future reports? (Indicate changes to organization, technical content, format, etc.) \_\_\_\_\_

CURRENT ADDRESS

Organization

Name E-mail Name

Street or P.O. Box No.

City, State, Zip Code

7. If indicating a Change of Address or Address Correction, please provide the Current or Correct address above and the Old or Incorrect address below.

OLD ADDRESS

Organization

Name

Street or P.O. Box No.

City, State, Zip Code

(Remove this sheet, fold as indicated, tape closed, and mail.) (DO NOT STAPLE)

---

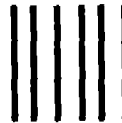
DEPARTMENT OF THE ARMY

OFFICIAL BUSINESS

**BUSINESS REPLY MAIL**  
FIRST CLASS PERMIT NO 0001, APG, MD

POSTAGE WILL BE PAID BY ADDRESSEE

DIRECTOR  
US ARMY RESEARCH LABORATORY  
ATTN AMSRL WM BC  
ABERDEEN PROVING GROUND MD 21005-5066



NO POSTAGE  
NECESSARY  
IF MAILED  
IN THE  
UNITED STATES

